European Review for Medical and Pharmacological Sciences 2020; 24: 4132-4144

Reduced long non-coding RNA PTENP1 contributed to proliferation and invasion *via* miR-19b/MTUS1 axis in patients with cervical cancer

L. OU[1,2], T.-Y. XIANG[1], X.-Y. HAO[1], D.-Z. WANG[3], Q. ZENG[1]

[1]Health Management Institute, The Second Medical Center and National Clinical Research Center for Geriatric Diseases, Chinese PLA General Hospital, Beijing, China
[2]Health Management Institute, The Zhengzhou People's Hospital, Zhengzhou, Henan, China
[3]Department of Traditional Chinese Medicine, Zhengzhou People's Hospital, Zhengzhou, Henan, China

Lei Ou and Tianyuan Xiang contributed to this work equally as co-first author

Abstract. – OBJECTIVE: Many studies showed that long non-coding RNAs (lncRNAs) may serve as prospective markers for patients with malignant cancers, including cervical cancer (CC). In this study, we mainly investigate the functions of lncRNA PTENP1 in the progression of human CC.

MATERIALS AND METHODS: Quantitative Real Time-Polymerase Chain Reaction (qRT-PCR) was performed to detect expression levels of PTENP1, miR-19b and MTUS1 in CC tissues, the adjacent tissues and CC cell lines. The correlations between PTENP1 with miR-19b, miR-19b with MTUS1 and PTENP1 with MTUS1 were analyzed. Overall survival (OS) of patients was analyzed using Kaplan-Meier method. Proliferation capacity was measured by CCK-8 assay and the invasion ability in CC cell line was detected by transwell assay. Western blot (WB) assay was performed to measure protein levels of tissues and CC cell lines. Finally, Dual-Luciferase reporter assay was performed to prove the potential binding sites between PTENP1 and miR-19b, miR-19b and MTUS1.

RESULTS: We found that PTENP1 was reduced in CC tissues and CC cell lines, which predicted the poor diagnosis of CC patients. MiR-19b was increased in CC tissues, which was negatively correlated with PTENP1 in CC tissues. MTUS1 was reduced in CC tissues, which was negatively correlated with miR-19b and positively correlated within PTENP1 CC tissues. Furthermore, PTENP1 overexpression inhibited cell proliferation ability and invasion capacity in HeLa cells, as well as repressed expressions of Cyclin D1, N-cadherin, and Vimentin. Moreover, Luciferase gene reporter assays verified that miR-19b was a direct target miRNA of PTENP1, and MTUS1 was identified as a direct target of miR-19b. In addition, the inhibited cell proliferation and invasion abilities in HeLa cells with p-PTENP1 were eliminated following with miR-19b mimic transfection.

CONCLUSIONS: According to the results, this study showed that PTENP1 was reduced in CC patients and it was a prognostic factor for CC patients. Furthermore, we firstly uncovered that PTENP1 could inhibit cell proliferation and invasion *via* miR-19b/MTUS1 in CC patients, which uncovered the tumor-suppressive role of PTENP1 in CC and suggested that it might be a potential target for treating human CC.

Key Words:
LncRNA PTENP1, MiR-19b, MTUS1, Invasion, Cervical cancer.

Introduction

Cervical cancer (CC) is one of the most common gynecological malignant cancers, which is the fourth cause of cancer-related death for women worldwide[1,2]. Although the incidence and mortality of CC patients are slowly decreasing due to the new treatments and improved diagnosis methods, the outcome and future survival rate remain unsatisfied[2-5]. It still needs more effort to make a better understanding and further explore the molecular mechanisms in the development of CC and find novel ways and therapeutic targets for treating human CC.

Long non-coding RNAs (lncRNAs) play important roles in biological functions of human diseases[6,7]. LncRNAs are classes of RNAs more than 200 nucleotides in length and have no capacity of protein-coding, but they are involved in many can-

Corresponding Author: Qiang Zeng, MD; e-mail: Zengqiang_301@163.com

cers[8-11]. Many lncRNAs play critical roles in the development and treatment resistance of CC[12-14]. PTENP1 is located at chromosome 9q13.3, which has been reported to be a tumor suppressor to repress tumor formation and development in some cancers[15-17]. PTENP1/miR200c axis was reported to inhibit PTEN in the development of endometrioid endometrial carcinoma[15]. Hao et al[16] reported that PTENP1 inhibited the tumor growth of esophageal squamous cell carcinoma by regulating SOCS6 expression and Gao et al[17] found that PTENP1 could regulate breast cancer progression by regulating PTEN. However, the function of PTENP1 in CC remained unknown.

MicroRNAs (miRNAs) play critical roles in diseases[18-20] by binding to the 3' untranslated regions (UTR) of downstream target genes, which are kinds of RNAs about 20-22 nucleotides in length. Tay et al[21] assumed that lncRNAs could affect the biological functions through lncRNA-miRNA-mRNA way, which was called mechanism of "competing endogenous RNA" (ceRNA)[22] and it was involved in various biological functions of cancers[23-25]. MiR-19b has been reported to play an oncogenic role that promoted cancer cell progression and resistance in many cancers[26-29]. Yuan et al[27] reported that miR-19b could suppress tumor cell apoptosis, promote proliferation, and induce tumorigenicity of multiple myeloma cells. Further, it was found that miR-19b could promote tumor progression *via* PI3K/AKT signaling pathway in breast cancer[28].

In this study, we firstly investigate the expressions of PTENP1 in CC tissues and we found that it was significantly decreased in CC tissues; as a result, we further explored the potential functions of PTENP1 in patients with CC.

Materials and Methods

Patients and Tissue Samples

A total of 56 pairs of CC tissues and adjacent non-tumor tissues were collected from patients in our hospital from May 2011 to October 2012. The patients were diagnosed with CC according to National Comprehensive Cancer Network (NCCN) Guidelines for Cervical Cancer[30]. Patients with no cardiac, blood system, liver or kidney diseases were included, and they did not receive any chemoradiotherapy before surgery. All tissues were cut into small pieces about 30-50 mg and were immediately frozen in liquid nitrogen at -80°C. Patients who received chemotherapy, radiotherapy or other treatments were excluded and all patients signed the informed consent. Our study was approved by the Faculty of Medicine's Ethics Committee of our hospital, which was performed according to the principles of the Declaration of Helsinki.

Cell Culture

Human normal cervical epithelium cell (HCvEpC) and human CC cell lines, such as Caski, C33A, SiHa and HeLa cells, were purchased from Type Culture Collection of the Chinese Academy of Sciences (Shanghai, China). The cells were cultured in Dulbecco's Modified Eagle's Medium (DMEM) medium (Gibco, Grand Island, NY, USA) supplemented with 10% fetal bovine serum (FBS; Gibco, Grand Island, NY, USA), 100 U/ml penicillin, and 100 μg/ml streptomycin. All cells were cultured in an appropriate incubator at 37°C and 5% CO_2.

Construction of Plasmids and Cell Transfection

The full length of human PTENP1 cDNA was synthesized and constructed into a plasmid (Invitrogen, Carlsbad, CA, USA), resulting with PTENP1 overexpression. MiR-19b mimic, miR-19b inhibitor, and miR-NC were purchased from RiBo Biotechnology (Guangzhou, China). The cells were pre-incubated on 6-well plates until reached about 60% confluence and cells were transfected with prepared plasmids or negative control (NC) or miR-19b mimic or miR-19b inhibitor with Lipofectamine 2000 (Invitrogen, Carlsbad, CA, USA) according to its instructions and cultured in an incubator at 37°C and 5% CO_2. At indicated time point after transfection, the cells were harvested for further study.

CCK-8 assays

Cell proliferation abilities were examined by using a Cell Counting Kit-8 (CCK-8, Dojindo Laboratories, Kumamoto, Japan) assay according to the protocol. HeLa cells were digested by 0.25% trypsin and seeded on 96-well plates with a concentration of 1×10^3 cells/ml and cultured at 37°C with 5% CO_2. For each well, 10 μl CCK-8 solution was added after cultivating for 1 d, 2 d and 3 d and incubated in darkness for another 4 h at 37°C with 5% CO_2. Finally, the optical density (OD) value was measured at 450 nm with microplate reader (Varioskan Flash, Thermo Fisher, Waltham, MA, USA) and cell proliferation curves were plotted. Each group was set with three replicate wells and three independent experiments were repeated to get the mean value.

Flow Cytometric Analysis of Cell Cycle

After transfection and other treatments, HeLa cells were digested with trypsin and washed twice by Phosphate-Buffered Saline (PBS); and cell precipitation was collected after centrifugation. Next, it was fixed with 75% ethanol at 4°C for about 4 h. After washed twice by cooled PBS, the cell pellet was stained with FITC-Annexin V and Propidium iodide (PI) at room temperature for 10 mins. The cells were measured by a FACSCalibur system (BD Pharmingen, San Diego, CA, USA) and analyzed by FlowJo software (Tree Star Corp, Ashland, OR, USA). Three independent experiments were repeated to get the mean value.

Transwell Assay

Cell invasion ability was measured by transwell assay. HeLa cells were put into the upper wells (5×10^4 cells/well) of transwell chamber on the non-coated membrane with 200 μl serum-free DMEM and 20 μl Matrigel (BD Biosciences, Franklin Lakes, NJ, USA) and DMEM with 10% fetal bovine serum (FBS) was added to the lower chambers, which were incubated at 37°C with 5% CO_2 for 24 h. After that, the liquid in the upper and lower chambers was abandoned and the non-invasive cells in the upper chambers were cleaned using cotton swab followed by PBS washing three times. Then, the invasive cells in the lower chamber were fixed and stained with methanol for 10 mins and stained with 0.1% crystal violet (Biyuntian, Shanghai, China). Finally, it was observed and counted using an inverted light microscope (Olympus Corporation, Tokyo, Japan). Three visual fields of a chamber were randomly chosen at least, and the invasive cells were counted. Three independent experiments were repeated to get the mean value.

RNA Extraction and Quantitative Real Time-PCR

Total RNA was extracted from human CC tissues, non-tumor adjacent tissues and human CC cell lines (Caski, C33A, SiHa and HeLa cells) using RNAiso Plus (TaKaRa, Otsu, Shiga, Japan) and purified by using GeneJET RNA Purification Kit (Thermo Fisher Scientific, Waltham, MA, USA) according to the protocols. Reverse transcription assay was performed using PrimeScript™ RT reagent Kit (TaKaRa, Otsu, Shiga, Japan) in accordance with the manufacturer's protocol and it was carried out in Reverse Transcription System A3500 (Promega, Madison, WI, USA). Gene primers were synthesized by Gene Pharma (Shanghai, China) and were listed in Table I. mRNA expressions were detected by SYBR Premix Ex Taq II (TaKaRa, Otsu, Shiga, Japan), which were normalized to GAPDH or U6 and $2^{-\Delta\Delta CT}$ method was used to calculate the relative mRNA expressions.

Protein Extraction and Western Blot (WB) Assay

Total proteins were extracted from human tissue samples and human CC cells by using a RIPA lysis buffer (Biyuntian, Shanghai, China) with proteinase inhibitor (Roche, Basel, Switzerland). Protein concentrations were measured by using a BCA kit (Pierce Chemical Co., Rockford, IL, USA). 40 ug proteins were added to 10% polyacrylamide gel electrophoresis (PAGE) and were separated. Then, the proteins were transferred onto polyvinylidene difluoride (PVDF) membranes and the membranes were incubated with primary antibodies overnight at 4°C. All primary antibodies were purchased from Abcam (Abcam, Cambridge, MA, USA), including MTUS1 (ab163572, 1:1000, 62 kDa), Cyclin D1 (ab134175, 1:10000, 34 kDa), N-cadherin (ab18203, 1:10000, 100 kDa), Vimentin (ab92547, 1:5000, 54 kDa), and E-cadherin (ab40772, 1:10000, 97 kDa), GAPDH (ab8245, 1:10000, 36 kDa). These membranes were subsequently incubated with matched secondary antibodies for 1 h at room temperature. Bio-Rad Gel Dol EZ Imager (Gel DocEZ Imager;

Table I. Primer sequences for qRT-PCR.

Gene names	Primer sequences
PTENP1	Forward: 5'-CCTGTTAAGAAAATGAGAAGACA-3' Reverse: 5'-TGTCCCTTATCAGATACATGACTTT-3'
MiR-16b	Forward: 5'-UGUGCAAAUCCAUGCAAAACUG-3' Reverse: 5'-GCTCACGCAACCTCCTCCTCC-3'
GAPDH	Forward: 5'-GGAGTCCACTGGTGTCTTCA-3' Forward: 5'-GGGAACTGAGCAATTGGTGG-3'
U6	Forward: 5'-CGCTTCGGCAGCACATATACT-3' Forward: 5'-CGCTTCACGAATTTGCGTGTC-3'

Bio-Rad, Hercules, CA, USA) was used to detect the protein bands. GAPDH was used as the internal reference and three independent experiments were repeated to get the mean value.

Dual-Luciferase Reporter Gene Assay

The segments containing the binding sites of miR-19b were constructed into GLO plasmids (Promega, Madison, WI, USA) with wild types PTENP1-wt and MTUS1-wt, mutant sequences PTENP1-mut and MTUS1-mut. The cells were seeded into 48-well plates (1×10^5 cells/well) and cultured for 24 h, then, the reporter gene plasmid and miR-19b mimic were co-transfected into the prepared cells according to Lipofectamine 2000 instructions for 24 h. GLO basic plasmids were mixed with Lipofectamine 2000 and DMEM medium for 30 mins, which were then transfected into former cells for other 24 h. Finally, a Promega Luciferase Assay (Promega, Madison, WI, USA) was used to measure the activities of firefly Luciferase and Renilla Luciferase according to the protocol and the relative Luciferase activity was normalized to the activity of Renilla Luciferase gene.

Statistical Analysis

Data were analyzed by Statistical Product and Service Solution 19.0 (IBM Corp., Armonk, NY, USA) and figures were graphed by GraphPad Prism 5.0 (GraphPad Software, La Jolla, CA, USA). Statistical significance was analyzed using Student's *t*-test, or One-way ANOVA and SNK method. Count data were processed by Chi-square test. Pearson's correlation analysis was used to analyze the gene correlations. Kaplan-Meier survival was used to analyze overall survival (OS) rate. If $p<0.05$, it was considered to be statistically significant.

Results

PTENP1 Was Reduced in CC Tissues and CC Cell Lines

To investigate the roles of PTENP1 in CC, we detected expressions of PTENP1 in 56 pairs of CC tissues and adjacent non-tumor tissues using qRT-PCR. The results showed that PTENP1 was significantly downregulated in CC tissues (Figure 1A) ($p<0.001$), compared to the adjacent non-tumor tissues. Furthermore, PTENP1 expression from patients at stage I-II was much lower than these from stage III-IV (Figure 1B) ($p<0.001$). Patients were divided into PTENP1 low expression group and high expression group and Kaplan-Meier survival analysis was performed. The results revealed that CC patients with PTENP1 low expression had a worse overall survival than the high expression group (Figure 1C) ($p<0.05$). Moreover, we analyzed the correlation between PTENP1 expression and clinicopathological features in CC patients. The results showed that the PTENP1 low expression was correlated with advanced FIGO stage, metastasis and recurrence (Table II) ($p<0.05$). In addition, to further explore the functions of PTENP1 in CC *in vivo*, we detected the PTENP1 expressions in human normal cervical epithelium cell line (HCvEpC) and human CC cell lines, including Caski, SiHa, C33A, and HeLa. The results showed that PTENP1 was reduced in CC cell lines (Figure 1D) ($p<0.05$), especially in HeLa cells; as a result, we used HeLa cells for further experiment. These data revealed that PTENP1 was reduced in CC tissues, which was correlated with the poor of CC patients. However, the functions of PTENP1 in CC remained unknown.

PTENP1 Overexpression Inhibited Cell Proliferation and Invasion in HeLa Cells

To explore the functions of PTENP1 in CC, plasmid PTENP1 (p-PTENP1) was constructed and resulted with PTENP1 overexpression. The plasmid was transfected into HeLa cells, and the results showed that PTENP1 was significantly upregulated (Figure 2A) ($p<0.001$). Then, CCK-8 assay was performed to measure the proliferation ability of HeLa cells. The results showed that PTENP1 overexpression inhibited cell proliferation, compared with p-NC (Figure 2B) ($p<0.01$). Furthermore, flow cytometry (FACS) revealed that PTENP1 overexpression inhibited cell growth by preventing cells from being in S phase and improving cell distribution in G0/G1 phase (Figure 2C) ($p<0.01$). Moreover, transwell assay indicated that PTENP1 overexpression could also inhibit cell invasion ability, compared with p-NC (Figure 2D) ($p<0.01$). In addition, WB was performed to detect the expressions of proliferation associated gene Cyclin D1 and invasion associated genes, including N-cadherin, Vimentin, and E-cadherin. The results revealed that Cyclin D1, N-cadherin, and Vimentin were repressed, while E-cadherin was increased (Figure 2E, F) ($p<0.01$), which indicated that the proliferation and invasion abilities were promoted. Collectively, these data suggested that overexpression of PTENP1 inhibited cell proliferation and invasion in HeLa cells.

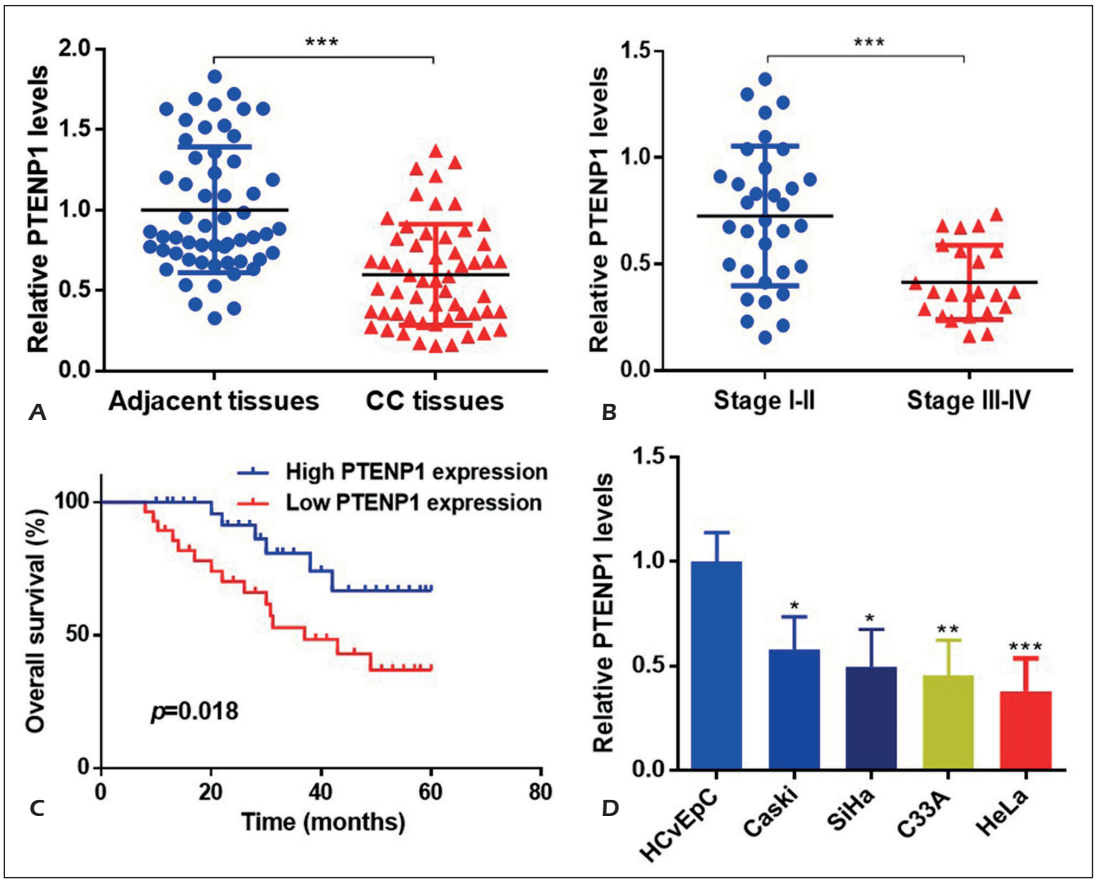

Figure 1. PTENP1 was reduced in CC tissues and CC cell lines. **A**, The expression of PTENP1 in CC tissues (n=56) and adjacent non-tumor tissues (n=56) was detected by qRT-PCR. **B**, The expression of PTENP1 in patients with stage I-II (n=33) and stage III-IV (n=23) was analyzed. **C**, Kaplan-Meier survival analysis was performed to analyze the overall survival of patients with PTENP1 high expression (n=28) and low expression (n=28). **D**, The expressions of PTENP1 in CC cell lines were detected by qRT-PCR. Data are shown as mean ± SD based on at least three independent experiments, *p<0.05, **p<0.01, ***p<0.001.

Table II. The relationships between PTENP1 and clinical parameters in CC patients.

Parameters	Low PTENP1 (n=28)	High PTENP1 (n=28)	*p*-value
Age			0.775
< 50	10	8	
≥ 50	18	20	
FIGO stage			**0.028**
I-II	12	21	
III-IV	16	7	
Lymphatic metastasis			**0.015**
Yes	18	8	
No	10	20	
Distant metastasis			**0.028**
Yes	16	7	
No	12	21	
Recurrence			**0.040**
Yes	9	2	
No	19	26	

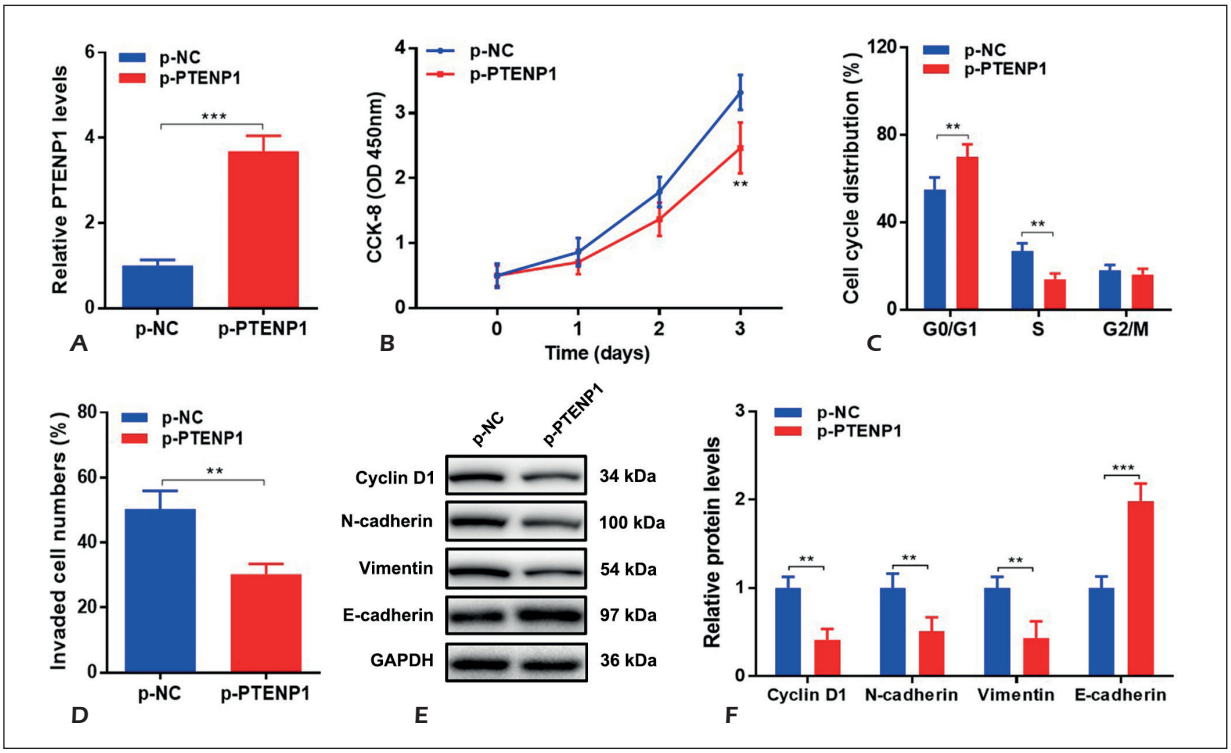

Figure 2. PTENP1 overexpression inhibited cell proliferation and invasion in HeLa cells. **A**, Expressions of PTENP1 were detected after transfecting p-PTENP1 or p-NC into HeLa cells. **B**, CCK-8 assay was performed to measure cell proliferation abilities. **C**, FACS was performed to evaluate the cell cycle distribution. **D**, Transwell assay was used to detected cell invasive abilities. **E-F**, The protein levels of Cyclin D1, N-cadherin, Vimentin and E-cadherin were detected by WB. Data are shown as mean ± SD based on at least three independent experiments, $^{**}p<0.01$, $^{***}p<0.001$.

MiR-19b Was Increased in CC Tissues and it Was Negatively Correlated with PTENP1

To further investigate the underlying mechanism that PTENP1 regulated tumor cell proliferation and invasion in CC, starBase v2.0 database was used and miR-19b was identified as a potential target miRNA of PTENP1. Then, we detected the expressions of miR-19b in CC tissues and its adjacent tissues. The results showed that miR-19b was significantly increased in CC tissues (Figure 3A) ($p<0.001$). Furthermore, miR-19b expression in patients at stage III-IV was much higher than these at stage I-II (Figure 3B) ($p<0.001$). Moreover, correlation analysis was performed, and results revealed that miR-19b was negatively correlated with PTENP1 in CC patients, especially in patients at the stage of III-IV (Figure 3C, D) ($p<0.001$). Besides, the expressions of miR-19b were significantly increased in CC cell lines, especially in HeLa cells (Figure 3E) ($p<0.001$). Additionally, we found that miR-19b was significantly decreased in HeLa cells transfected with p-PTENP1, compared to p-NC (Figure 3F) ($p<0.001$). Collectively, these data indicated that PTENP1 was negatively interacted with miR-19b and it was predicted as a target miRNA of PTENP1 (Figure 3G). To confirm whether PTENP1 could function as a ceRNA to competitively bind with miR-19b, PTENP1 wild type and PTENP1 mutant sequences were constructed into GLO vectors and the Luciferase reporter assay was performed. The results showed that the relative Luciferase activity in HeLa cells co-transfected with PTENP1-wt and miR-19b mimic was significantly repressed compared with that in the cells transfected with miR-NC. Furthermore, the Luciferase activity was reversed in cells co-transfected with PTENP1-mut and miR-19b mimic (Figure 3H) ($p<0.01$). Similar results were found in 293 cells (Figure 3I) ($p<0.01$). These results suggested that PTENP1 could directly bind with miR-19b in CC and HeLa cells.

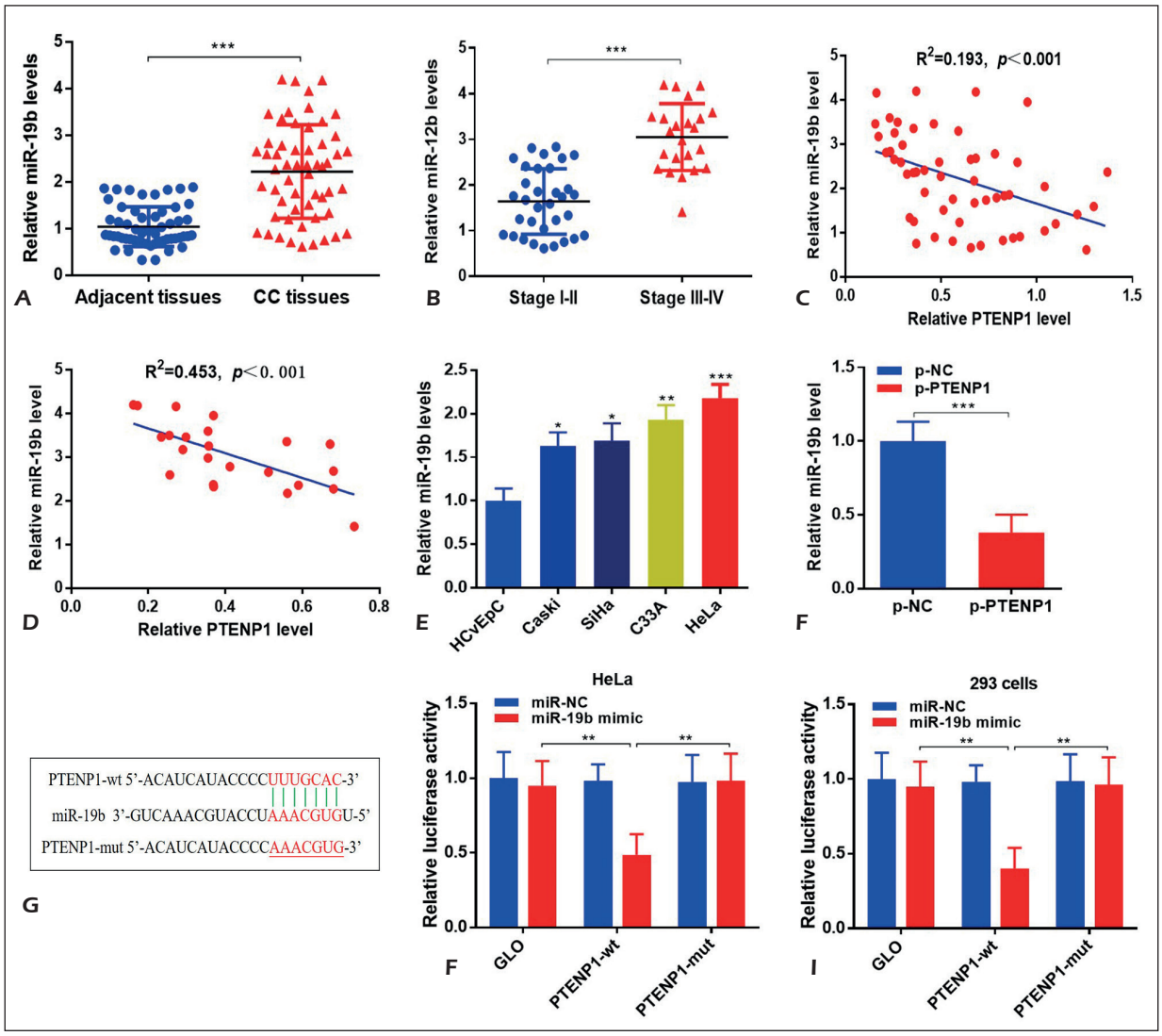

Figure 3. MiR-19b was increased in CC tissues and it was negatively correlated with PTENP1. **A**, The expression of miR-19b in CC tissues (n=56) and adjacent non-tumor tissues (n=56) were detected by RT-PCR. **B**, The expression of miR-19b in patients with stage I-II (n=33) and stage III-IV (n=23) were analyzed. **C-D**, Correlations between PTENP1 and miR-19b were analyzed using correlation analysis. **E**, MiR-19b levels in CC cell lines were detected by qRT-PCR. **F**, MiR-19b levels were detected by RT-PCR in HeLa cells transfected with p-PTENP1 or p-NC. **G**, Potential wild type binding sequence and mutant sequence of PTENP1 and miR-19b were constructed. **H-I**, Luciferase gene reporter assay was performed to verify the binding site in HeLa cells and 293 cells. Data are shown as mean ± SD based on at least three independent experiments, *p<0.05, **p<0.01, ***p<0.001.

MiR-19b Regulated Cell Proliferation and Invasion in HeLa Cells

To further explore the functions of miR-19b in CC, the miR-19b mimic or miR-19b inhibitor or miR-NC was respectively transfected into HeLa cells. The results showed that miR-19b was significantly increased after miR-19b mimic transfection (Figure 4A) (p<0.001), while it was significantly repressed after miR-19b inhibitor transfection (Figure 4A) (p<0.001). CCK-8 assay revealed that the cell proliferation ability was repressed and was followed by miR-19b inhibition, while it was improved following miR-19b overexpression (Figure 4B) (p<0.01). FACS assay showed that cell distribution in G0/G1 phase was improved following miR-19b inhibition, while it was repressed following miR-19b overexpression (Figure 4C) (p<0.001). Transwell assay revealed that miR-19b inhibition significantly inhibited cell invasion, while miR-19b overexpression drastically promoted cell invasion ability (Figure 4D) (p<0.01). Besides, proliferation associated gene

Cyclin D1 and invasion associated genes were detected by WB. The results showed that Cyclin D1, N-cadherin, Vimentin were repressed and E-cadherin was increased following miR-19b inhibition, while it showed the opposite results following miR-19b overexpression (Figure 4E, F) (p<0.01). Collectively, these data suggested that miR-19b regulated cell proliferation and invasion in HeLa cells. However, the detailed mechanism of miR-19b in CC cells remained unknown.

MiR-19b Directly Targeted at MTUS1 and it was Positively Correlated with PTENP1

To make a better understanding of how miR-19b regulated tumor cell proliferation and invasion, we used TargetScan database and MTUS1 was identified as a target gene, which was reported to be associated with cell proliferation and tumorigenesis in some cancers[31-33]. As a result, we detected the protein expressions of MTUS1 in CC tissues and the adjacent tissues. The results showed that MTUS1 was significantly decreased in CC tissues (Figure 5A) (p<0.001). Furthermore, MTUS1 levels in patients at stage III-IV was much lower than these at stage I-II (Figure 5B) (p<0.001). Moreover, Correlation analysis revealed that miR-19b was negatively correlated with MTUS1 in CC patients (Figure 5C) (p<0.01), especially in patients at stage of III-IV (Figure 5D) (p<0.001). Besides, MTUS1 was positively correlated with PTENP1 in CC patients (Figure 5E) (p<0.01) and in patients at stage of III-IV (Figure 5F) (p<0.001). Additionally, MTUS1 protein levels in CC cell lines were increased, especially in HeLa cells (Figure 5G) (p<0.001). MTUS1 was increased following PTENP1 overexpression (Figure 5H) (p<0.001), it was repressed following miR-19b overexpression, while it was increased following miR-19b inhibition (Figure 5H, I) (p<0.01). Above all, these results indicated that miR-19b was negatively interacted with MTUS1,

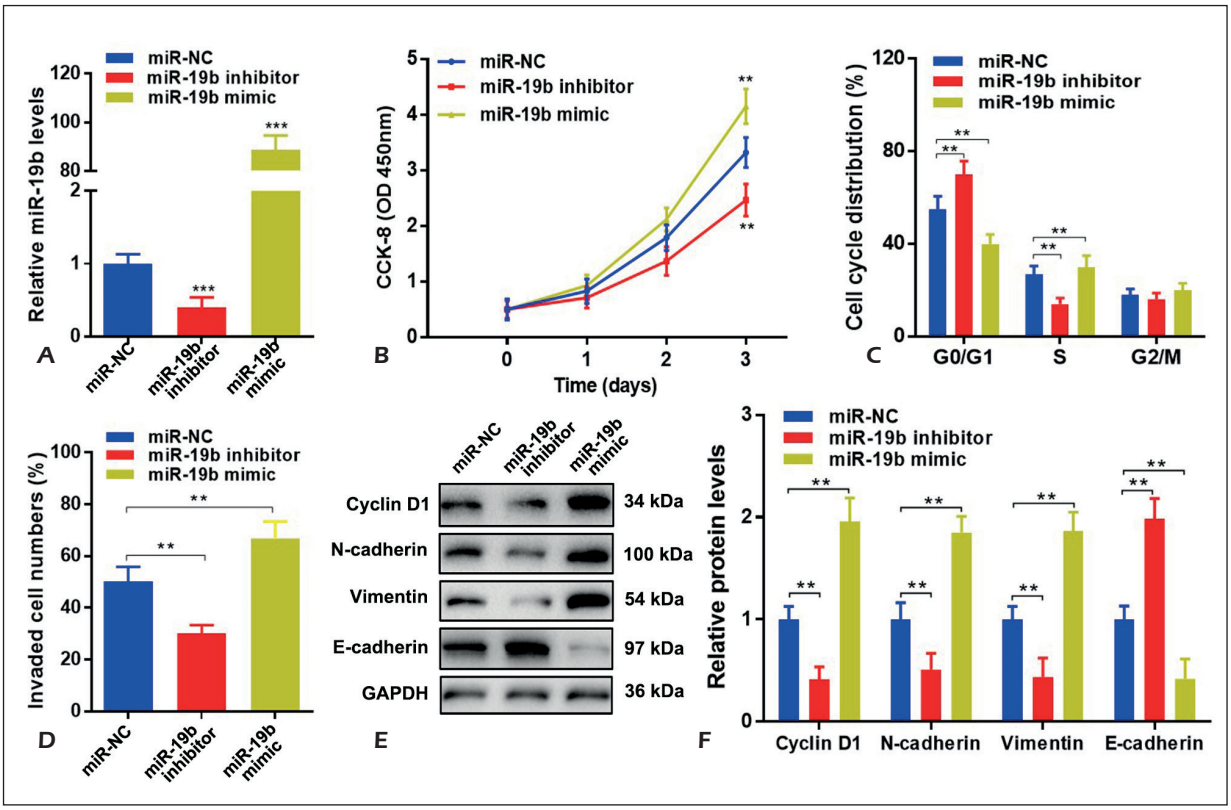

Figure 4. MiR-19b regulated cell proliferation and invasion in HeLa cells. **A**, The expressions of miR-19b were detected in HeLa cells after transfecting with the miR-19b mimic or miR-19b inhibitor or miR-NC. **B**, Cell proliferation abilities of indicated HeLa cells were measured by CCK-8 assay. **C**, FACS was performed to evaluate cell cycle distribution. **D**, Transwell assay was used to detected cell invasive abilities. **E-F**, The protein levels of Cyclin D1, N-cadherin, Vimentin and E-cadherin were detected by WB. Data are shown as mean ± SD based on at least three independent experiments, **p<0.01, ***p<0.001.

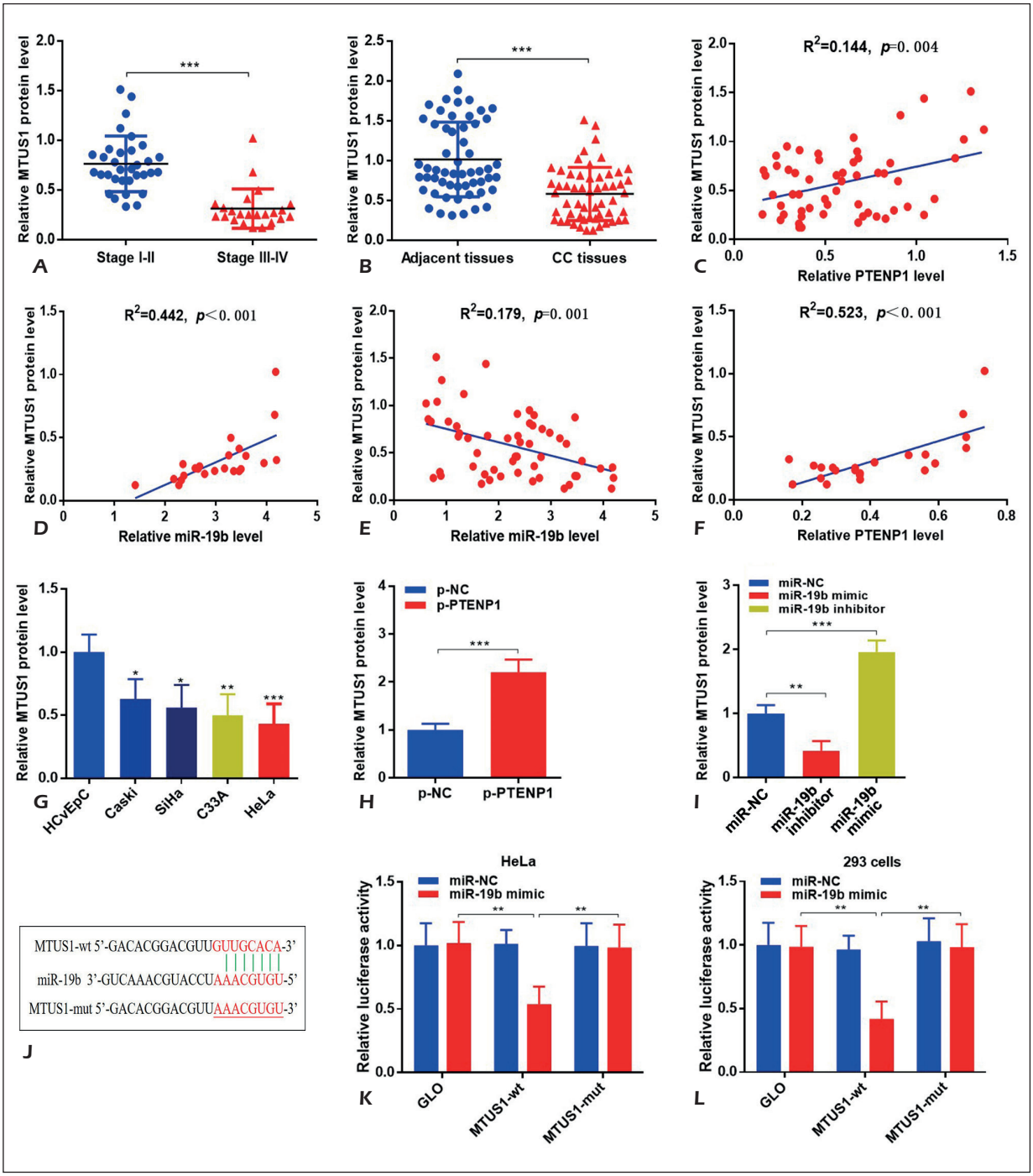

Figure 5. MiR-19b directly targeted at MTUS1 and it was positively correlated with PTENP1. **A**, The protein levels of MTUS1 in CC tissues (n=56) and adjacent non-tumor tissues (n=56) were detected. **B**, The MTUS1 levels in patients with stage I-II (n=33) and stage III-IV (n=23) were analyzed. **C-F**, Correlations between MTUS1 with miR-19b, miR-19b with PTENP1 were analyzed using correlation analysis. **G**, MTUS1 protein levels in CC cell lines were detected by WB. H, MTUS1 levels were detected in HeLa cells transfected with p-NC or p-PTENP1 by WB. I, MTUS1 levels were detected in HeLa cells transfected with miR-NC or miR-19b mimic or miR-19b inhibitor. **J**, Potential wild type binding sequence and mutant sequence of MTUS1 and miR-19b were constructed. **K-L**, Luciferase gene reporter assay was performed to verify the binding site in HeLa cells and 293 cells. Data are shown as mean ± SD based on at least three independent experiments, *p<0.05, **p<0.01, ***p<0.001.

which was also predicted as a target gene of miR-19b. To verify whether it could target MTUS1 in CC, MTUS1-wt and MTUS1-mut sequences were constructed into GLO vectors (Figure 5J) and Luciferase gene reporter assay was performed. The results demonstrated that the overexpression of miR-19b significantly attenuated the Luciferase activity of MTUS1-wt but not that of MTUS1-mut vector in HeLa cells and 293 cells (Figure 5K, L) (p<0.01). Collectively, these results suggested that miR-19b could directly target MTUS1 and it was positively correlated with PTENP1. As a result, we might assume that PTENP1 could sponge with miR-19b, which directly repressed MTUS1 expression and regulated cell proliferation and invasion of CC patients.

PTENP1 Inhibited Proliferation and Invasion Via miR-19b/MTUS1 Axis in HeLa Cells

To verify the assumption, miR-19b mimic or miR-NC was respectively transfected into HeLa cells with p-PTENP1. After transfecting miR-19b mimic into HeLa cells with p-PTENP1, the repressed miR-19b levels and promoted PTENP1 levels were reversed (Figure 6A) (p<0.001). Furthermore, the repressed cell proliferation ability and invasion ability were also reversed (Figure 6B, D) (p<0.001). Moreover, FACS assay showed that the improved cell distribution in G0/G1 phase was reduced following with miR-19b mimic transfection into HeLa cells with p-PTENP1 (Figure 6C) (p<0.01). Additionally, WB assay revealed that the repressed protein levels of MTUS1, Cyclin D1, N-cadherin, and Vimentin were improved, while the promoted E-cadherin level was reduced following miR-19b mimic transfection into HeLa cells with p-PTENP1 (Figure 6E, F) (p<0.01). Collectively, these results suggested that PTENP1 might inhibit proliferation and invasion via miR-19b/MTUS1 in CC patients and HeLa cells.

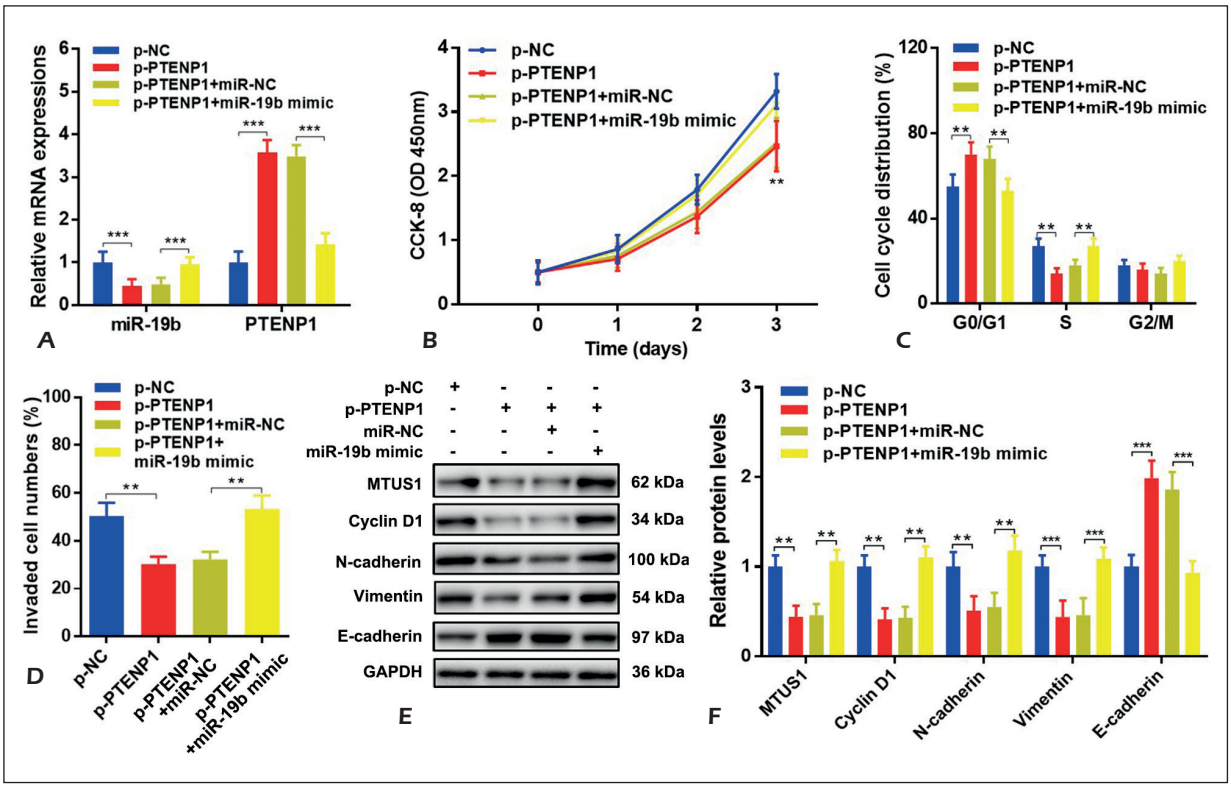

Figure 6. PTENP1 inhibited proliferation and invasion *via* miR-19b/MTUS1 axis in HeLa cells. **A**, The mRNA levels of miR-19b and PTENP1 were detected in HeLa cells after co-transfecting with miR-19b mimic and p-PTENP1. **B**, Cell proliferation abilities of indicated HeLa cells were measured by CCK-8 assay. **C**, FACS was performed to evaluate cell cycle distribution. **D**, Transwell assay was used to detected cell invasive abilities. **E-F**, The protein levels of MTUS1, Cyclin D1, N-cadherin, Vimentin and E-cadherin were detected by WB. Data are shown as mean ± SD based on at least three independent experiments, **p<0.01, ***p<0.001.

Discussion

LncRNAs are crucial regulators during biological processes and functions in diseases[6,7], especially in various kinds of human cancers[8-11]. Recent studies[15-17] found that PTENP1 was involved in repressing the development of some cancers. However, whether it played some roles in CC remained unknown. As a result, for the first time, we detected the expressions of PTENP1 in CC tissues and adjacent non-tumor tissues. We demonstrated that PTENP1 was significantly decreased in CC tissues, which was correlated with advanced FIGO stage, metastasis and recurrence of patients. Furthermore, we also detected the expressions of PTENP1 in CC cell lines, and the results showed that PTENP1 was reduced, especially in HeLa cells.

To investigate the functions of PTENP1 in CC, p-PTENP1 was constructed and transfected into HeLa cells. PTENP1 was significantly increased after p-PTENP1 transfection. The PTENP1 overexpression inhibited cell proliferation and invasion abilities, as well as inhibited cell growth by improving cell distribution in G0/G1 phase. Cyclin D1 is associated with cell proliferation in various cancers[34-36]. Epithelial-mesenchymal transition (EMT) is a process in which epithelial cells are transformed into cells with mesenchymal phenotype and the cell adhesion molecules are decreased, playing important roles in promoting metastasis of malignant tumors, such as CC[37,38]. Invasion associated genes, including N-cadherin and Vimentin, play an important role in promoting tumor cell invasion in cancers[39-41]. We found that these genes were repressed following with PTENP1 overexpression. However, the detail underlying mechanism remained unknown.

MiRNAs have been reported to play critical roles in diseases by sponging lncRNAs[21,22] and miRNAs are involved in various biological functions of cancers[23-25]. To further explore the mechanism that PTENP1 regulated tumor cell proliferation and invasion in CC, starBase v2.0 database was used and miR-19b was identified as a potential target miRNA of PTENP1, which was reported to be an oncogenic gene in many cancers[26-29]. We found that miR-19b was significantly increased in CC tissues and CC cell lines, which was negatively correlated with PTENP1 in CC patients. Further, it was remarkably repressed following PTENP1 overexpression. The Luciferase gene reporter assay demonstrated that PTENP1 could directly sponge miR-19b in HeLa cells and 293 cells. To further explore the functions of miR-19b in CC, the miR-19b mimic or miR-19b inhibitor was respectively transfected into HeLa cells. The results showed that the cell proliferation ability and invasion were repressed following with miR-19b inhibition, while they were reversed following with miR-19b overexpression.

To further explore the mechanism of miR-19b regulated tumor cell proliferation and invasion, TargetScan database was used and MTUS1 was identified as a target gene, which was associated with cell proliferation and tumorigenesis in some cancers[31-33]. Then, we found that MTUS1 was reduced in CC tissues and cell lines, and was negatively correlated with miR-19b and was positively correlated with PTENP1 in CC patients. The Luciferase gene reporter assay confirmed that miR-19b could directly bind MTUS1 in CC. Thus, we might assume that PTENP1 could sponge miR-19b, which directly targeted the repression of MTUS1 expression and regulated cell proliferation and invasion of CC patients. Finally, to verify that assumption, miR-19b mimic was transfected into HeLa cells with p-PTENP1. We found that the repressed cell proliferation ability and invasion ability were also reversed following miR-19b overexpression. Collectively, these results showed that PTENP1 inhibited cell proliferation and invasion *via* miR-19b/MTUS1 axis in CC patients.

Conclusions

Above all, our study detected that PTENP1 was reduced in CC patients and it was a prognostic factor for CC patients. Furthermore, we firstly uncovered that PTENP1 could inhibit cell proliferation and invasion *via* miR-19b/MTUS1 in CC patients, which uncovered the tumor-suppressive role of PTENP1 in CC and suggested that it might be a potential target for treating human CC.

Conflict of Interests

The authors declare that they have no conflict of interest.

Funds

This investigation was funded by 1. N-glycan profiling as a risk stratification biomarker for type II diabetes. The Funds for International Cooperation and Exchange of the National Natural Science Foundation of China (General Program). Grant No. 81561128020; 2. The mechanism of menaquinones-based gut microbiota symbiosis and effect on diabetes. The National Natural Science Foundation of China (General Program). Grant No. 81872920.

References

1) Vaccarella S, Lortet-Tieulent J, Plummer M, Franceschi S, Bray F. Worldwide trends in cervical cancer incidence: impact of screening against changes in disease risk factors. Eur J Cancer 2013; 49: 3262-3273.
2) Siegel R L, Miller K D, Jemal A. Cancer statistics, 2016. CA Cancer J Clin 2016; 66: 7-30.
3) Miller KD, Siegel RL, Lin CC, Mariotto AB, Kramer JL, Rowland JH, Stein KD, Alteri R, Jemal A. Cancer treatment and survivorship statistics, 2016. CA Cancer J Clin 2016; 66: 271-289.
4) Ventriglia J, Paciolla I, Pisano C, Cecere SC, Di Napoli M, Tambaro R, Califano D, Losito S, Scognamiglio G, Setola SV, Arenare L, Pignata S, Della Pepa C. Immunotherapy in ovarian, endometrial and cervical cancer: state of the art and future perspectives. Cancer Treat Rev 2017; 59: 109-116.
5) Torre LA, Sauer AM, Chen MS, Kagawa-Singer M, Jemal A, Siegel RL. Cancer statistics for Asian Americans, Native Hawaiians, and Pacific Islanders, 2016: converging incidence in males and females. CA Cancer J Clin 2016; 66: 182-202.
6) Hauptman N, Glavac D. MicroRNAs and long non-coding RNAs: prospects in diagnostics and therapy of cancer. Radiol Oncol 2013; 47: 311-318.
7) Morris KV, Mattick JS. The rise of regulatory RNA. Nat Rev Genet 2014; 15: 423-437.
8) Sun Z, Zhang C, Wang T, Shi P, Tian X, Guo Y. Correlation between long non-coding RNAs (lncRNAs) H19 expression and trastuzumab resistance in breast cancer. J Cancer Res Ther 2019; 15: 933-940.
9) Qi L, Zhang T, Yao Y, Zhuang J, Liu C, Liu R, Sun C. Identification of lncRNAs associated with lung squamous cell carcinoma prognosis in the competitive endogenous RNA network. PeerJ 2019; 7: e7727.
10) Zhu J, Chen S, Yang B, Mao W, Yang X, Cai J. Molecular mechanisms of lncRNAs in regulating cancer cell radiosensitivity. Biosci Rep 2019; 39. pii: BSR20190590.
11) Huang Q R, Pan X B. Prognostic lncRNAs, miRNAs, and mRNAs form a competing endogenous RNA network in colon cancer. Front Oncol 2019; 9: 712.
12) Luo W, Wang M, Liu J, Cui X, Wang H. Identification of a six lncRNAs signature as novel diagnostic biomarkers for cervical cancer. J Cell Physiol 2020; 235: 993-1000.
13) Huang J, Liu T, Shang C, Zhao Y, Wang W, Liang Y, Guo L, Yao S. Identification of lncRNAs by microarray analysis reveals the potential role of lncRNAs in cervical cancer pathogenesis. Oncol Lett 2018; 15: 5584-5592.
14) Peng L, Yuan X, Jiang B, Tang Z, Li GC. LncRNAs: key players and novel insights into cervical cancer. Tumour Biol 2016; 37: 2779-2788.
15) Chen R, Zhang M, Liu W, Chen H, Cai T, Xiong H, Sheng X, Liu S, Peng J, Wang F, Chen H, Lin W, Xu X, Zheng W, Jiang Q. Estrogen affects the negative feedback loop of PTENP1-miR200c to inhibit PTEN expression in the development of endometrioid endometrial carcinoma. Cell Death Dis 2018; 10: 4.
16) Hao SC, Ma H, Niu ZF, Sun SY, Zou YR, Xia HC. hUC-MSCs secreted exosomes inhibit the glioma cell progression through PTENP1/miR-10a-5p/PTEN pathway. Eur Rev Med Pharmacol Sci 2019; 23: 10013-10023.
17) Gao X, Qin T, Mao J, Zhang J, Fan S, Lu Y, Sun Z, Zhang Q, Song B, Li L. PTENP1/miR-20a/PTEN axis contributes to breast cancer progression by regulating PTEN via PI3K/AKT pathway. J Exp Clin Cancer Res 2019; 38: 256.
18) Rahman MM, Brane AC, Tollefsbol TO. MicroRNAs and epigenetics strategies to reverse breast cancer. Cells 2019; 8. pii: E1214.
19) Bartel DP. MicroRNAs: target recognition and regulatory functions. Cell 2009; 136: 215-233.
20) Khan AQ, Ahmed EI, Elareer NR, Junejo K, Steinhoff M, Uddin S. Role of miRNA-regulated cancer stem cells in the pathogenesis of human malignancies. Cells 2019; 8. pii: E840.
21) Salmena L, Poliseno L, Tay Y, Kats L, Pandolfi PP. A ceRNA hypothesis: the Rosetta Stone of a hidden RNA language? Cell 2011; 146: 353-358.
22) Tay Y, Kats L, Salmena L, Weiss D, Tan SM, Ala U, Karreth F, Poliseno L, Provero P, Di Cunto F, Lieberman J, Rigoutsos I, Pandolfi PP. Coding-independent regulation of the tumor suppressor PTEN by competing endogenous mRNAs. Cell 2011; 147: 344-357.
23) Li Q, Yu Q, Ji J, Wang P, Li D. Comparison and analysis of lncRNA-mediated ceRNA regulation in different molecular subtypes of glioblastoma. Mol Omics 2019; 15: 406-419.
24) Liang W, Sun F. Identification of pivotal lncRNAs in papillary thyroid cancer using lncRNA-mRNA-miRNA ceRNA network analysis. Peer J 2019; 7: e7441.
25) Zhao L, Hu K, Cao J, Wang P, Li J, Zeng K, He X, Tu PF, Tong T, Han L. LncRNA miat functions as a ceRNA to upregulate sirt1 by sponging miR-22-3p in HCC cellular senescence. Aging (Albany NY) 2019; 11: 7098-7122.
26) Zhang TJ, Lin J, Zhou JD, Li XX, Zhang W, Guo H, Xu ZJ, Yan Y, Ma JC, Qian J. High bone marrow miR-19b level predicts poor prognosis and disease recurrence in de novo acute myeloid leukemia. Gene 2018; 640: 79-85.
27) Yuan J, Su Z, Gu W, Shen X, Zhao Q, Shi L, Jin C, Wang X, Cong H, Ju S. MiR-19b and miR-20a suppress apoptosis, promote proliferation and induce tumorigenicity of multiple myeloma cells by targeting PTEN. Cancer Biomark 2019; 24: 279-289.
28) Li C, Zhang J, Ma Z, Zhang F, Yu W. MiR-19b serves as a prognostic biomarker of breast cancer and

promotes tumor progression through PI3K/AKT signaling pathway. Onco Targets Ther 2018; 11: 4087-4095.

29) Song M, Sun M, Xia L, Chen W, Yang C. MiR-19b-3p promotes human pancreatic cancer Capan-2 cells proliferation by targeting phosphatase and tension homolog. Ann Transl Med 2019; 7: 236.

30) Koh WJ, Greer BE, Abu-Rustum NR, Apte SM, Campos SM, Cho KR, Chu C, Cohn D, Crispens MA, Dorigo O, Eifel PJ, Fisher CM, Frederick P, Gaffney DK, Han E, Huh WK, Lurain JR, Mutch D, Fader AN, Remmenga SW, Reynolds RK, Teng N, Tillmanns T, Valea FA, Yashar CM, McMillian NR, Scavone JL. Cervical cancer, version 2.2015. J Natl Compr Canc Netw 2015; 13: 395-404.

31) Kara M, Kaplan M, Bozgeyik I, Ozcan O, Celik OI, Bozgeyik E, Yumrutas O. MTUS1 tumor suppressor and its miRNA regulators in fibroadenoma and breast cancer. Gene 2016; 587: 173-177.

32) Gu Y, Liu S, Zhang X, Chen G, Liang H, Yu M, Liao Z, Zhou Y, Zhang CY, Wang T, Wang C, Zhang J, Chen X. Oncogenic miR-19a and miR-19b co-regulate tumor suppressor MTUS1 to promote cell proliferation and migration in lung cancer. Protein Cell 2017; 8: 455-466.

33) Xiao J, Chen JX, Zhu YP, Zhou LY, Shu QA, Chen LW. Reduced expression of MTUS1 mRNA is correlated with poor prognosis in bladder cancer. Oncol Lett 2012; 4: 113-118.

34) Hamzeloo-Moghadam M, Aghaei M, Abdolmoham Madi MH, Fallahian F. Anticancer activity of britannin through the downregulation of cyclin D1 and CDK4 in human breast cancer cells. J Cancer Res Ther 2019; 15: 1105-1108.

35) Mountzios G, Kotoula V, Kolliou GA, Papadopoulou K, Lazaridis G, Christodoulou C, Pentheroudakis G, Skondra M, Koutras A, Linardou H, Razis E, Papakostas P, Chrisafi S, Aravantinos G, Nicolaou I, Goussia A, Kalogeras K, Pectasides D, Fountzilas G. Cyclin D1 differential activation and its prognostic impact in patients with advanced breast cancer treated with trastuzumab. ESMO Open 2019; 4: e441.

36) Zhong Q, Hu Z, Li Q, Yi T, Li J, Yang H. Cyclin D1 silencing impairs DNA double strand break repair, sensitizes BRCA1 wildtype ovarian cancer cells to olaparib. Gynecol Oncol 2019; 152: 157-165.

37) Jiang C, Xu R, Li XX, Wang YY, Liang WQ, Zeng JD, Zhang SS, Xu XY, Yang Y, Zhang MY, Wang HY, Zheng XFS. p53R2 overexpression in cervical cancer promotes AKT signaling and EMT, and is correlated with tumor progression, metastasis and poor prognosis. Cell Cycle 2017; 16: 1673-1682.

38) Qureshi R, Arora H, Rizvi MA. EMT in cervical cancer: its role in tumor progression and response to therapy. Cancer Lett 2015; 356: 321-331.

39) Silva RS, Lombardi APG, de Souza DS, Vicente CM, Porto CS. Activation of estrogen receptor beta (ERbeta) regulates the expression of N-cadherin, E-cadherin and beta-catenin in androgen-independent prostate cancer cells. Int J Biochem Cell Biol 2018; 96: 40-50.

40) Casal JI, Bartolome RA. Beyond N-cadherin, relevance of cadherins 5, 6 and 17 in cancer progression and metastasis. Int J Mol Sci 2019; 20. pii: E3373.

41) Mrozik KM, Blaschuk OW, Cheong CM, Zannettino ACW, Vandyke K. N-cadherin in cancer metastasis, its emerging role in haematological malignancies and potential as a therapeutic target in cancer. BMC Cancer 2018; 18: 939.